PHYSICAL REVIEW E **77**, 041403 (2008)

Energy dissipation of a Brownian particle in a viscoelastic fluid

Shoichi Toyabe[1,2,*] and Masaki Sano[1,†]
[1]*Department of Physics, Graduate School of Science, University of Tokyo, Hongo, Tokyo 113-0033, Japan*
[2]*Department of Physics, Faculty of Science and Engineering, Chuo University, Kasuga, Tokyo 112-8551, Japan*

(Received 7 February 2008; published 15 April 2008; publisher error corrected 1 May 2008)

We evaluate the energy dissipation rate of an optically driven Brownian particle in a polymer solution utilizing the generalized version of Harada and Sasa's equality [Phys. Rev. Lett. **95**, 130602 (2005)] by Deutsch and Narayan [Phys. Rev. E **74**, 026112 (2006)]. The irreversible work of a small system is estimated from readily obtainable quantities. By adopting the time-dependent memory function obtained by microrheology measurement, directly obtained works are in excellent agreement with those calculated from the generalized fluctuation dissipation theorem for nonequilibrium steady states. This result implies that the colloidal particle in a polymer solution can be described by the generalized Langevin equation.

DOI: 10.1103/PhysRevE.77.041403 PACS number(s): 82.70.−y, 05.40.Jc, 87.80.Cc, 05.70.Ln

I. INTRODUCTION

Energy dissipation rate is an important quantity to characterize the nonequilibrium steady states. However, it is usually hard to measure it by experiments in small fluctuating systems. Recently, Harada and Sasa derived an equality, which enables us to calculate the energy dissipation rate from readily obtainable quantities by experiments such as the correlation function and the response function of the velocity [1–4]. This equality was originally derived for the Markovian systems described by the Langevin equation. On the other hand, systems which are more practical often have retarded friction. For example, molecular motors are working in extremely crowded environment in cells. In such a situation, non-Markovian behavior is expected. Also, microrheological systems, such as a Brownian particle in a polymer solution or colloid suspension, are recently attracting extensive studies including nonequilibrium physics [5,6]. A particle moving in such a fluid feels a retarded friction. If this is the case, the following generalized Langevin equation (GLE) [7] has been used as the model equation

$$\int_{-\infty}^{t} \gamma(t-s)\dot{x}(s)ds = -\frac{\partial U(x,t)}{\partial x} + F(t) + \hat{\xi}(t), \qquad (1)$$

where $x(t)$ is, for example, the position of a Brownian particle. $U(x,t)$ is the potential energy. $F(t)$ is the external force. $\hat{\xi}(t)$ is the thermal force. $\gamma(t-s)$ is a time-dependent frictional coefficient, which accounts for the memory effect. The origin of this memory is the past motion of the particle itself, or a reflection. In a polymer solution, the particle's motion changes the conformation of the polymer network, which results in the aftereffect for the future motion of the particle. This is not expected in a pure viscous fluid such as water except in a very high frequency region. The fluctuation dissipation theorem of the second type [8] relates the thermal fluctuation $\hat{\xi}(t)$ to the friction coefficient $\gamma(t)$ as $\langle\hat{\xi}(t)\hat{\xi}(s)\rangle = k_B T\gamma(t-s)$. $\gamma(t)$ does no longer have a white spectrum but a "colored" one, which has a frequency dependence.

In 2006, Deutsch and Narayan extended Harada and Sasa's equality to systems described by the GLE [9],

$$\langle J_0\rangle = \int_{-\infty}^{\infty} \frac{d\omega}{2\pi}\tilde{\gamma}'(\omega)[v_s^2 + \tilde{C}(\omega) - 2k_B T\tilde{R}'(\omega)], \qquad (2)$$

where J is the energy dissipation rate. Fourier transform of an arbitrary function $A(t)$ is defined as $\tilde{A}(\omega) \equiv \int_{-\infty}^{\infty} A(t)\exp(i\omega t)dt$. $\tilde{A}'(\omega)$ denotes the real part of $\tilde{A}(\omega)$. $C(t)$ is the autocorrelation function of the velocity, $C(t) \equiv \langle[\dot{x}(t)-v_s][\dot{x}(0)-v_s]\rangle_0$, where $v_s \equiv \langle\dot{x}(t)\rangle_0$ is the steady-state velocity. $R(t)$ is the linear response function of the velocity to a small external probe force $\varepsilon f^p(t)$,

$$\langle\dot{x}(t)\rangle_\varepsilon - v_s = \varepsilon\int_{-\infty}^{t} R(t-s)f^p(s)ds + o(\varepsilon^2), \qquad (3)$$

where $\langle\cdots\rangle_\varepsilon$ denotes an ensemble average under the probe force $f^p(t)$ of order ε. Although it is usually a hard task to measure $\langle J\rangle$ in small systems by experiments, $\tilde{C}(\omega)$ and $\tilde{R}'(\omega)$ are usually more accessible than $J(t)$. In the original form of Harada and Sasa's equality, $\tilde{\gamma}'(\omega)$ was independent of ω. Note that the right-hand side of Eq. (2) vanishes near the equilibrium state due to the fluctuation dissipation theorem (FDT) [8] of the first kind, $\tilde{C}(\omega) = 2k_B T\tilde{R}'(\omega)$, while it has a finite value in nonequilibrium states generally. Thus the equality implies the direct relation between the energy dissipation rate and the FDT violation. The local equality at each frequency is also expected,

$$\tilde{I}(\omega) = \tilde{\gamma}'(\omega)[v_s^2 + \tilde{C}(\omega) - 2k_B T\tilde{R}'(\omega)], \qquad (4)$$

where $\tilde{I}(\omega)$ is the real part of the Fourier transform of the cross correlation $I(t)$ of the force and velocity,

$$I(t) \equiv \frac{\langle F(x(t),t)\circ v(0)\rangle_0 + \langle F(x(0),0)\circ v(t)\rangle_0}{2}. \qquad (5)$$

In this paper, we evaluated the energy dissipation rate of an optically driven colloidal particle in a polymer solution using Eqs. (2) and (4).

---

[*] toyabe@phys.chuo-u.ac.jp

[†] sano@phys.s.u-tokyo.ac.jp

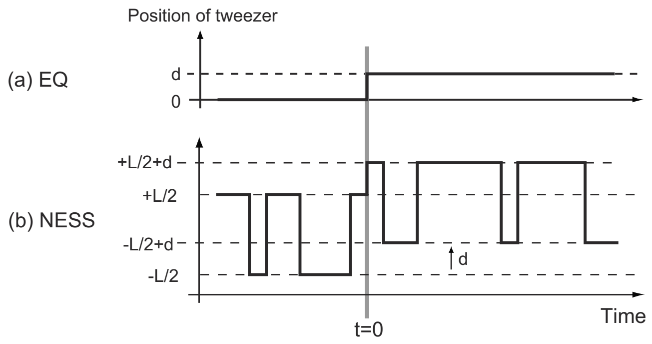

FIG. 1. Measurement of response function. (a) We shifted the tweezer position with a distance of $d=72.2$ nm at $t=0$ and observed the relaxation processes to the new tweezer position. We repeated this and obtained an ensemble average. (b) Similarly in nonequilibrium steady states (NESSs), we added a bias d and observed the relaxation processes.

II. MATERIALS AND METHODS

The experimental setup and procedure were almost the same as those in the previous study [4]. We suspended a particle (carboxylated polystyrene particle with a diameter of 0.984 ± 0.023 μm (polysciences)] in a 1.0 wt % polyethylene oxide (PEO) solution. PEO is a nonionic polymer studied extensively in macrorheological [10] and microrheological [11–15] experiments. The molecular weight of the PEO we used ranges from 1 500 000 Da to 2 000 000 Da (WAKO), which corresponds to a length from 11.5 μm to 15.3 μm. We dissolved PEO in ultrapure autoclaved water with a final concentration of 1.0 wt %. At this concentration, polymers are expected to form an entangled network with an average mesh size of 14.9 nm [14,16]. An antibiotic Ampicillin was added with a final volume fraction of 0.1% to suppress the growth of contaminated bacteria. We trapped a particle in this PEO solution by the optical tweezer method. The particle image was captured by a charge coupled device (CCD) camera (Hamamatsu, HISCA C6770) at 472 Hz. The distance between the particle and the bottom glass surface, which is the nearest wall of the chamber from the trapped particle, was around 12 μm. This is enough to eliminate the interaction of the particle with the glass surface. The temperature was kept at 21.6 ± 0.1 °C.

To drive the system to nonequilibrium steady states (NESSs), we trapped a particle by an optical tweezer and swinged the trapping position between two sites at random in time [4]. This was achieved by a Piezo mounted mirror (PI, S-226) controlled by a personal computer. The correlation function was obtained from the trajectory of the particle position. To know the response function, we shifted the position of the tweezer a small amount horizontally ($d=72.2$ nm) and observed the relaxation phenomena to the new tweezer position (Fig. 1). The corresponding probe force $\varepsilon f^p(t)$ changed from $0(t<0)$ to $kd(t\geqslant 0)$, where k is the spring constant of the optical tweezer.

We obtained the complex friction coefficient $\tilde{\gamma}(\omega)$ as the following. In the equilibrium state, the fluctuation dissipation theorem gives

$$\tilde{C}_x(\omega) \equiv \langle|\tilde{x}(\omega)|^2\rangle = \frac{2k_B T\tilde{\alpha}''(\omega)}{\omega}, \tag{6}$$

where $\tilde{C}_x(\omega)$ is the power spectrum density of the particle position. The complex compliance $\tilde{\alpha}(\omega)$ is defined as the linear response of a sphere embedded in an isotropic medium and subjected to an oscillatory force [17]: $\tilde{x}(\omega)=\tilde{\alpha}(\omega)\tilde{f}(\omega)$. Thus, for a particle trapped in the harmonic potential with a spring constant k,

$$\tilde{\alpha}(\omega) = \frac{1}{i\omega\tilde{\gamma}(\omega)+k}. \tag{7}$$

For a linear response coefficient with causality, the following Kramers-Kronig relation connects the real part and imaginary part of that as

$$\tilde{\alpha}'(\omega) = \frac{2}{\pi}P\int_0^\infty \frac{\zeta\tilde{\alpha}''(\zeta)}{\zeta^2-\omega^2}d\zeta, \tag{8}$$

where P is Cauthy's principal of the complex integral. Thus, provided that $\tilde{C}_x(\omega)$ is known over a wide enough frequency range, the Kramers-Kronig relation enables us to calculate $\tilde{\alpha}'(\omega)$. Especially, the integral in Eq. (8) can be rewritten as

$$\frac{2}{\pi}P\int_0^\infty \frac{\zeta\tilde{\alpha}''(\zeta)}{\zeta^2-\omega^2}d\zeta = \frac{2}{\pi}\int_0^\infty dt\cos\omega t\int_0^\infty d\zeta\tilde{\alpha}''(\zeta)\sin\zeta t. \tag{9}$$

Therefore, methods based on Fourier transform are applicable to calculate $\tilde{\alpha}'(\omega)$. Thus, from the power spectrum density of the particle position $\langle|\tilde{x}(\omega)|^2\rangle$, we can calculate the complex friction coefficients using Eqs. (6)–(8) [17,18].

III. RESULTS

A. Spring constant

At first, we trapped a particle with fixing the position of the tweezer and obtained a histogram of the particle location

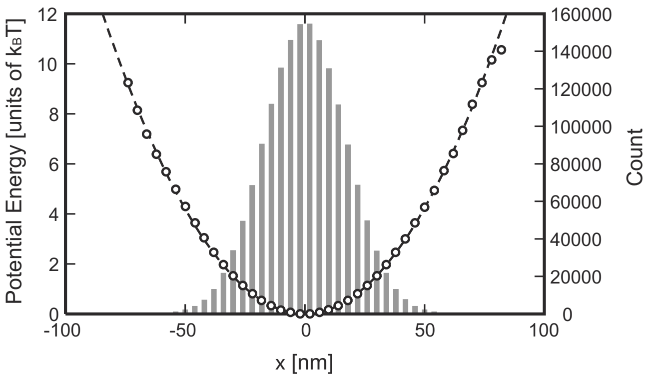

FIG. 2. Histogram of particle positions trapped in a single fixed tweezer and the corresponding potential profile estimated using the Boltzmann distribution. The number of the total count was 1 015 777. The dashed line is the fitting curve of the harmonic function $U(x)=(1/2)kx^2$ with a spring constant of $k=3373\pm 8k_BT/\mu\text{m}^2=13.72\pm 0.03$ pN/μm.

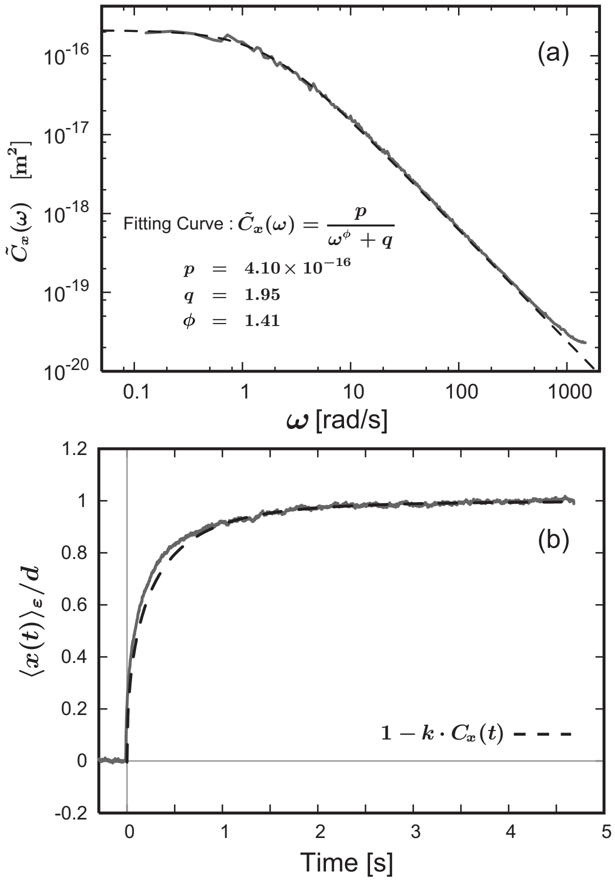

FIG. 3. (a) The correlation function of the particle position. 51 trajectories of 69.1 s were averaged. The dashed line is a fitting curve $p/(\omega^\phi + q)$ with $p = 4.10\times 10^{-16}$, $q = 1.96$, $\phi = 1.41$. The rising of the spectrum in the high frequency region (>1000 rad/s) is due to the systematic error and aliasing effect. The data were smoothed with an exponentially increasing window. (b) Relaxation curve in equilibrium state (EQ). We transferred the tweezer position a small amount ($d = 72.2$ nm) and observed the relaxation process to the new tweezer position. 1040 of 5 s trajectories were averaged. The dashed line is the inverse Fourier-Cos transform of the fitted line in (a), which corresponds to $1 - kC_x(t)$. The shape of the relaxation curve can be well fitted by a stretched exponential function (data not shown), $\langle x(t)\rangle_\varepsilon / d = 1 - \exp[-(t/\tau)^\beta]$ with $\beta = 0.494 \pm 0.002$ and $\tau = 0.169 \pm 0.001$ s.

(Fig. 2). From that, we recovered the potential profile, which was well fitted by a harmonic potential $U(x) = (1/2)kx^2$ with a spring constant of $k = 3373 \pm 8 k_B T/\mu\text{m}^2 = 13.72 \pm 0.03$ pN/μm.

B. Fluctuation dissipation theorem

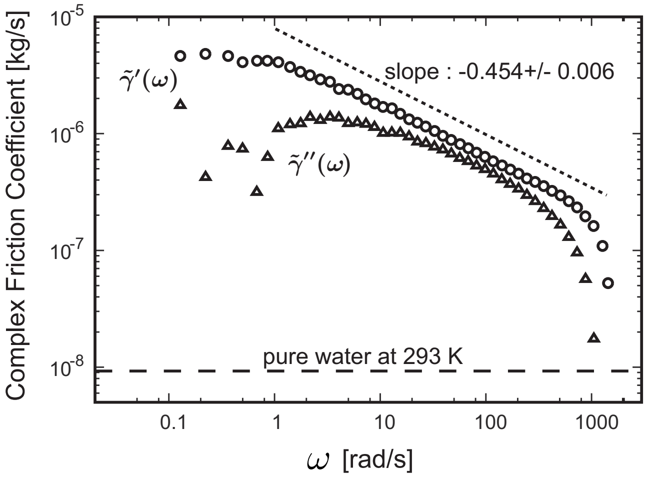

FIG. 4. The complex friction coefficient $\tilde{\gamma}(\omega) \equiv \tilde{\gamma}'(\omega) - i\tilde{\gamma}''(\omega)$. The steep drop of values in the high frequency region is due to our insufficient bandwidth for $\tilde{C}_x(\omega)$. The dashed line is the friction coefficient for pure water 9.273×10^{-9} kg/s at 20 °C for a particle with a diameter of around 1 μm. The dotted line is a fitting curve for $\tilde{\gamma}'(\omega)$ in a frequency region from 10 to 300 rad/s, which had a slope of -0.454 ± 0.006.

We checked the fluctuation dissipation theorem in the equilibrium state. The correlation function of the particle position in the equilibrium state, in which the position of the tweezer was fixed, is shown in Fig. 3(a). With an analogy of the case in a viscous fluid, we fitted the data by a function similar to a Lorentzian,

$$\tilde{C}_x(\omega) \equiv \langle |\tilde{x}(\omega)|^2 \rangle = \frac{p}{\omega^\phi + q}, \tag{10}$$

where $p = 4.10\times 10^{-16}$, $q = 1.96$, and $\phi = 1.41$. For a particle trapped in a pure viscous fluid, ϕ is exactly 2. Thus, we found that a particle in a PEO solution shows a different spectrum from that in a pure viscous fluid.

The dashed line in Fig. 3(b) was the relaxation curve calculated from the fitting curve in Fig. 3(a) by an inverse Fourier-Cos transform, which coincided well with the relaxation curve in the equilibrium state. Thus, we verified the

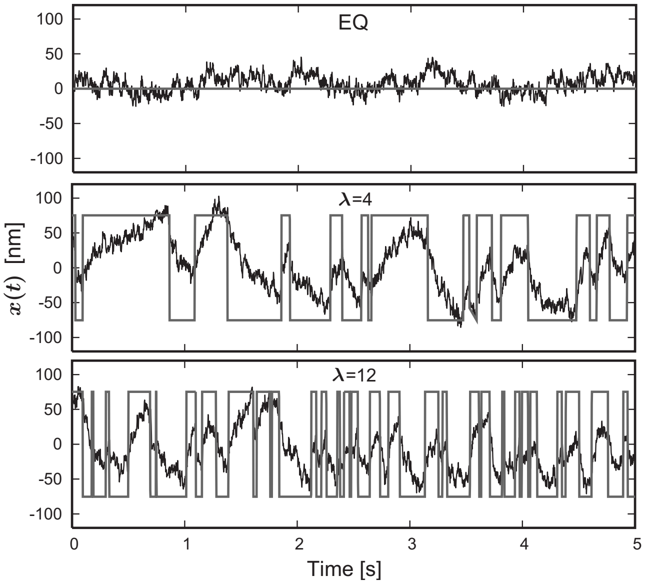

FIG. 5. Typical trajectories for EQ and NESSs with switching rates of λ=4 and 12 events/s. Black lines are trajectories of the particle. Gray lines are trajectories of the tweezer.

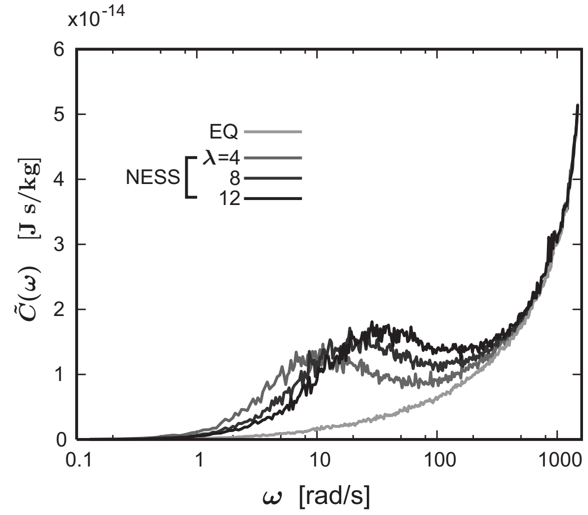

FIG. 6. The correlation function of the velocity $\tilde{C}(\omega)$. We see that $\tilde{C}(\omega)$ in NESSs have higher spectrum than that in EQ. In the high frequency region, they converged to the same curve. We averaged 51 trajectories of 69.1 s each for each curve. The data were smoothened with an exponentially increasing window.

fluctuation dissipation theorem of the first kind for the particle position in the equilibrium state. Note that the relaxation curve in Fig. 3(b) was not an exponential function as in the case in a viscous fluid [4], but was well fitted by a stretched exponential curve (data not shown), $\langle x(t)\rangle_\varepsilon / d = 1 - \exp[-(t/\tau)^\beta]$ with $\beta = 0.494 \pm 0.002$ and $\tau = 0.169 \pm 0.001$ s.

C. Complex friction coefficient

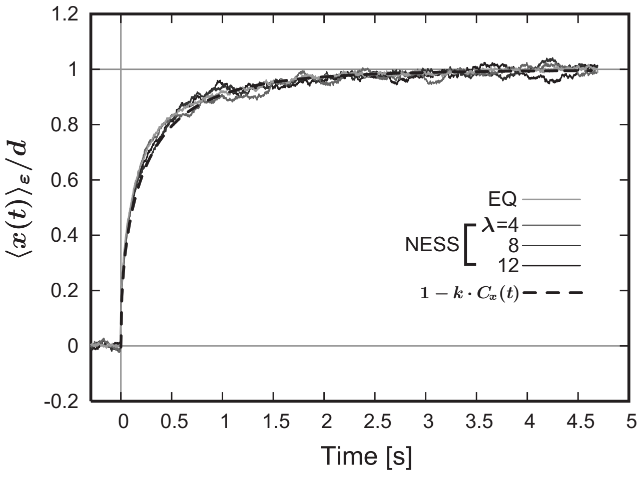

FIG. 7. Relaxation curves in equilibrium state (EQ) and nonequilibrium states (NESSs). The dashed line is the same as that in Fig. 3(b). We transferred the tweezer position a small amount ($d = 72.2$ nm) and observed the relaxation process to the new tweezer position. 1040 of 5 s trajectories were averaged for each curve. We found that relaxation curves for EQ and NESSs coincided well.

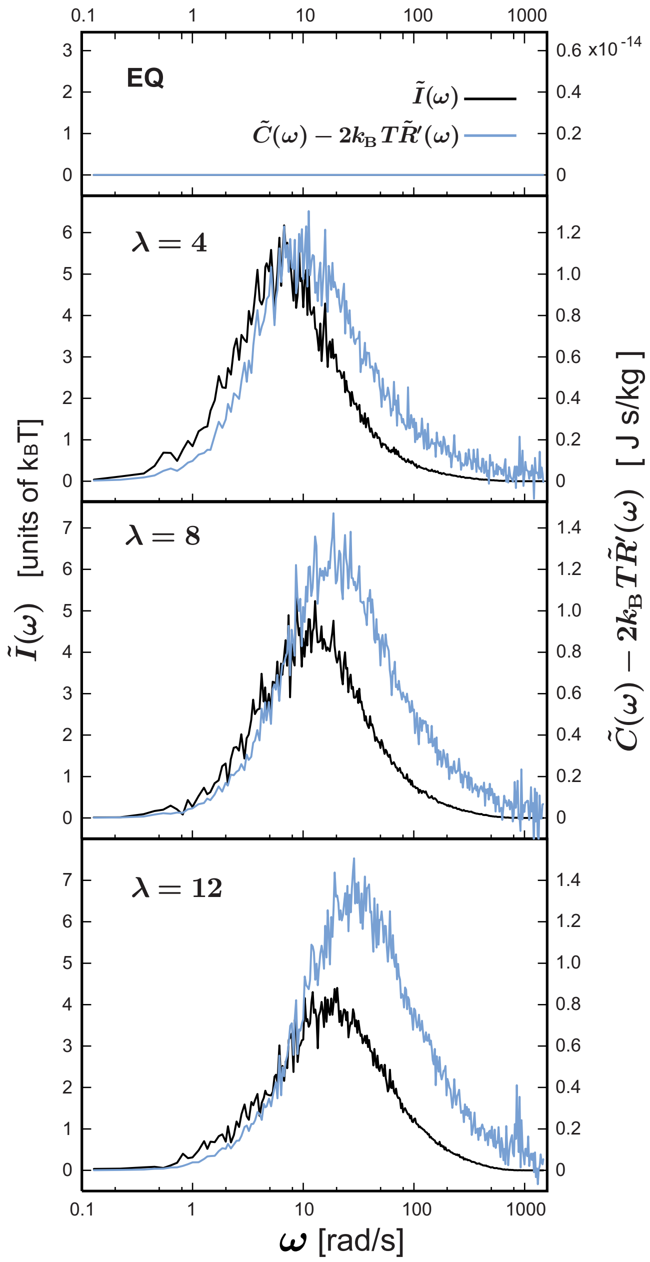

FIG. 8. (Color online) $\tilde{I}(\omega)$ (black) vs $\tilde{C}(\omega) - 2k_B T\tilde{R}'(\omega)$ (blue). We plotted $\tilde{C}(\omega) - \tilde{C}_{EQ}(\omega)$ instead of $\tilde{C}(\omega) - 2k_B T\tilde{R}'(\omega)$ (see the main text). We found a significant deviation in the shape of them. The left and right vertical axes are for $\tilde{I}(\omega)$ and $\tilde{C}(\omega) - 2k_B T\tilde{R}'(\omega)$, respectively.

According to the procedure described in Sec. II, we calculated the complex friction coefficient. In Fig. 4(a) we found that $\tilde{\gamma}'(\omega)$ and $\tilde{\gamma}''(\omega)$ now depend on the frequency ω in contrast to the case in a pure viscous fluid. $\tilde{\gamma}'(\omega)$ had a bent around 1 rad/s. And, in the intermediate region, the slope of $\tilde{\gamma}'(\omega)$ was -0.454 ± 0.006 (dotted line). In the high frequency region, we had a steep drop due to our limited bandwidth.

D. Nonequilibrium steady states

We switched the position of the optical tweezer temporally between two sites at random in a Poissonian process

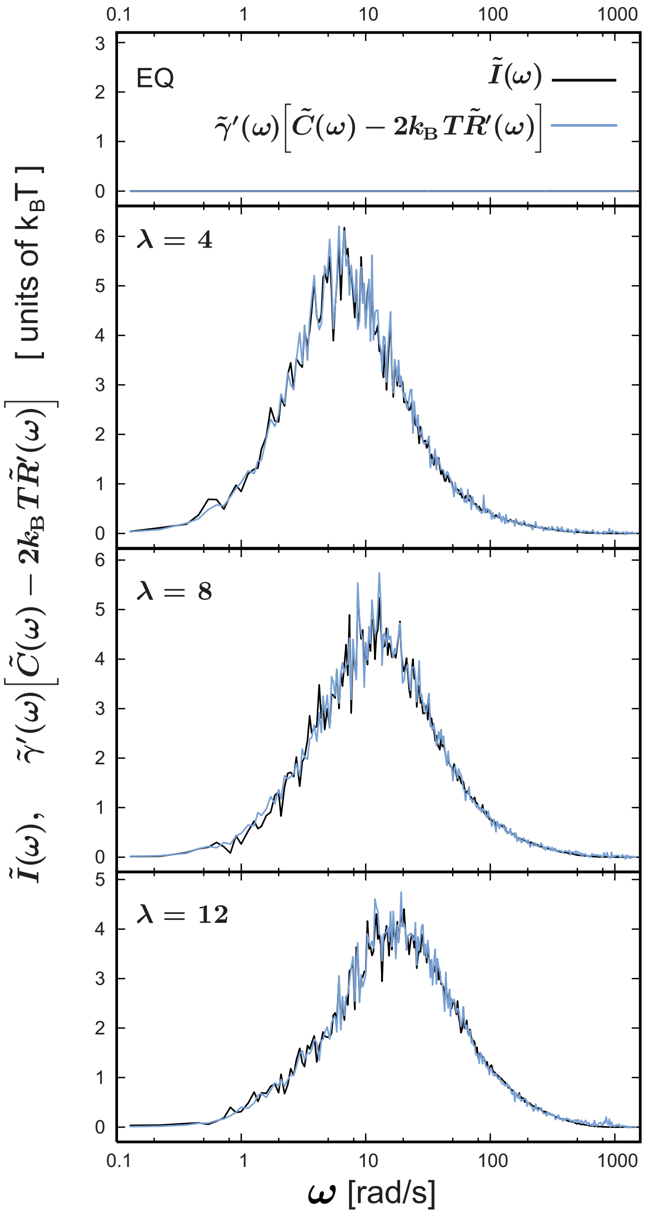

FIG. 9. (Color online) Both sides of the local equality [Eq. (4)] at each frequency. $\tilde{I}(\omega)$ (black) vs $\tilde{\gamma}'(\omega)$ $[\tilde{C}(\omega)-2k_BT\tilde{R}'(\omega)]$ (blue).

(see [4] for details) to construct nonequilibrium steady states (NESSs). We showed typical trajectories in the equilibrium state (EQ) and NESSs with switching rates of $\lambda=4$ and 12 events/s in Fig. 5. In the equilibrium state, the particle was wandering around the tweezer. On the other hand, it was swinged by the switching tweezer in nonequilibrium state. In Fig. 6, we showed the correlation function of the velocity $\tilde{C}(\omega)$. Note that the steady velocity $v_s \equiv \langle \dot{x}(t) \rangle$ is expected to be zero. We found that the correlation functions in NESSs are different from that in EQ. Also, positions of peaks increased as the switching rate increased. On the other hand, relaxation curves in EQ and NESSs (Fig. 7) coincided well.

E. Energy dissipation rate

As we have seen in the previous section, we confirmed the fluctuation dissipation relation in EQ (Fig. 3). Also, we found that response functions in EQ and NESSs were the same in Fig. 7. Therefore, we evaluated the equality using the difference between $\tilde{C}(\omega)$ in NESSs and that in EQ: $\tilde{C}(\omega)-\tilde{C}_{\mathrm{EQ}}(\omega)$ instead of $\tilde{C}(\omega)-2k_BT\tilde{R}'(\omega)$, where $\tilde{C}_{\mathrm{EQ}}(\omega)$ is the correlation function in EQ. This procedure reduces systematic noise. In Fig. 8, we showed this difference $\tilde{C}(\omega)-\tilde{C}_{\mathrm{EQ}}(\omega)$ and $\tilde{I}(\omega)$ [Eq. (4)]. Since the potential profile of the optical tweezer is known, we can calculate the left-hand side of Eq. (4), $\tilde{I}(\omega)$, using Eq. (5). The whole shapes were significantly different between them. However, after the multiplications of $\tilde{\gamma}'(\omega)$, they had a good coincidence (Fig. 9). Thus, we confirmed the local equality at each frequency to a good extent. We found that the position of the peak moved to a high frequency region when we increased the switching rate. On the contrary, the height of the peak decreased. We had some deviation between two values in the high frequency region. This is probably the error due to the aliasing effect of the discrete Fourier transform and some systematic noise. Finally, the integrated version of the equality [Eq. (2)] was shown in Fig. 10. Since the high frequency region was disturbed by the aliasing effect and systematic noise, we integrated both sides of the equality up to a frequency of 400 rad/s. Both sides of the equality had an excellent coincidence within the statistical error. The error bars were smaller than the size of the marks.

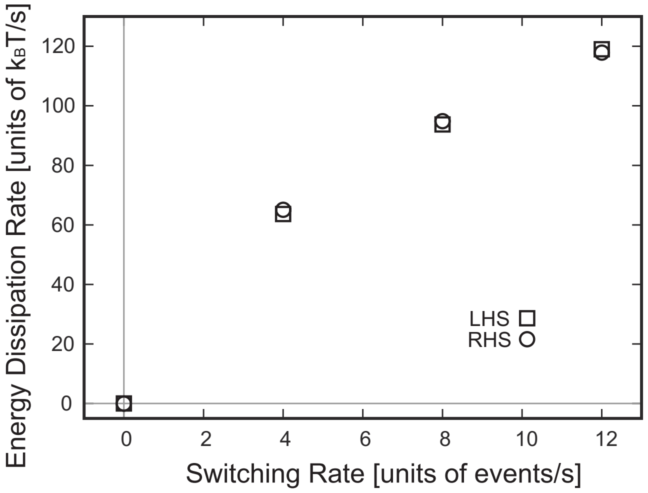

FIG. 10. The left-hand side (squares) and right-hand side (circles) of Deutsch and Narayan's equality [Eq. (2)] were plotted against the switching rate. We have integrated both sides of the equality up to a frequency of 400 rad/s to avoid artifactual noise at high frequency (see the main text). For the right-hand side, we used $\tilde{C}_{\mathrm{EQ}}(\omega)$ instead of $2k_BT\tilde{R}'(\omega)$. The error bars were smaller than the size of the marks.

Although the height of the peaks decreased with the switching rates (Fig. 9), the width of the peaks increase. This resulted in the increase of energy dissipation (Fig. 10).

IV. CONCLUSION

In a polymer solution, we evaluated the energy dissipation rate for an optically trapped colloid under nonequilibrium steady states using Deutsch and Narayan's equality, which is the generalization of Harada and Sasa's equality derived for the generalized Langevin equation. We measured the frequency-dependent complex friction coefficient $\tilde{\gamma}(\omega)$, the correlation function of the velocity $\tilde{C}(\omega)$, and the response function of the velocity $\tilde{R}(\omega)$. As a result, we evaluated the energy dissipation rate to a good extent within a statistical error without knowing the detail of the system such as the force profile using this equality.

The Deutsch and Narayan's generalization [Eq. (2)] is a theorem which holds as the identical relation for the generalized Langevin equations [7]. In this sense, our results imply the validity of the description of our system by the GLE. In some systems, the description by the GLE was confirmed experimentally [19]. For a Brownian particle embedded in a polymer solution, the GLE has been utilized to model the system [11]. Indeed, the friction term in the GLE has a simple and reasonable form for the extension of the Langevin equation to include the memory effect. However, as far as we know, the description of such a system (a Brownian particle in a viscoelastic fluid) by the GLE has not been established experimentally. This experiment would be evidence of that.

ACKNOWLEDGMENTS

We appreciate helpful suggestions of Takao Ohta, Takahiro Ohkuma, Shin-ichi Sasa, Takahiro Harada, and Akira Shimizu. This work was supported by the Ministry of Education, Science, Sports, and Culture of Japan (Grant Nos. 16206020 and 18068005).

[1] T. Harada and S.-I. Sasa, Phys. Rev. Lett. **95**, 130602 (2005).
[2] T. Harada and S.-I. Sasa, Phys. Rev. E **73**, 026131 (2006).
[3] H. Teramoto and S.-I. Sasa, Phys. Rev. E **72**, 060102(R) (2005).
[4] S. Toyabe, H. R. Jiang, T. Nakamura, Y. Murayama, and M. Sano, Phys. Rev. E **75**, 011122 (2007).
[5] T. Ohkuma and T. Ohta, J. Stat. Mech.: Theory Exp. (2007) P10010.
[6] T. Speck and U. Seifert, J. Stat. Mech.: Theory Exp. (2007) L09002.
[7] H. Mori, Prog. Theor. Phys. **33**, 423 (1965).
[8] R. Kubo, M. Toda, and N. Hashitsume, *Statsitical Physics II*, 2nd ed. (Springer, Berlin, 1991).
[9] J. M. Deutsch and O. Narayan, Phys. Rev. E **74**, 026112 (2006).
[10] D. M. Yu, G. L. Amidon, N. D. Weiner, and A. H. Goldberg, J. Pharm. Sci. **83**, 1443 (1994).
[11] T. G. Mason and D. A. Weitz, Phys. Rev. Lett. **74**, 1250 (1995).
[12] T. G. Mason, K. Ganesan, J. H. van Zanten, D. Wirtz, and S. C. Kuo, Phys. Rev. Lett. **79**, 3282 (1997).
[13] G. Popescu, A. Dogariu, and R. Rajagopalan, Phys. Rev. E **65**, 041504 (2002).
[14] B. R. Dasgupta, S.-Y. Tee, J. C. Crocker, B. J. Frisken, and D. A. Weitz, Phys. Rev. E **65**, 051505 (2002).
[15] Q. Lu and M. J. Solomon, Phys. Rev. E **66**, 061504 (2002).
[16] K. Devanand and J. C. Selser, Macromolecules **24**, 5943 (1991).
[17] M. J. Solomon and Q. Lu, Curr. Opin. Colloid Interface Sci. **6**, 430 (2001).
[18] B. Schnurr, F. Gittes, F. C. MacKintosh, and C. F. Schmidt, Macromolecules **30**, 7781 (1997).
[19] R. P. Ojha, P. A. Lemieux, P. K. Dixon, A. J. Liu, and D. J. Durian, Nature (London) **427**, 521 (2004).